Supplementary Materials

March 4, 2025

A The impacts of parameter on the performance of SMO-STANet

A.1 The impacts of parameter *n_heads* on the performance of SMO-STANet

we have conducted experiments to evaluate the impacts of parameter *n_heads* on the performance of SMO-STANet to determine their optimal values. According to the Figure 1, we set *n_heads* to 8 to achieve the optimal performance.

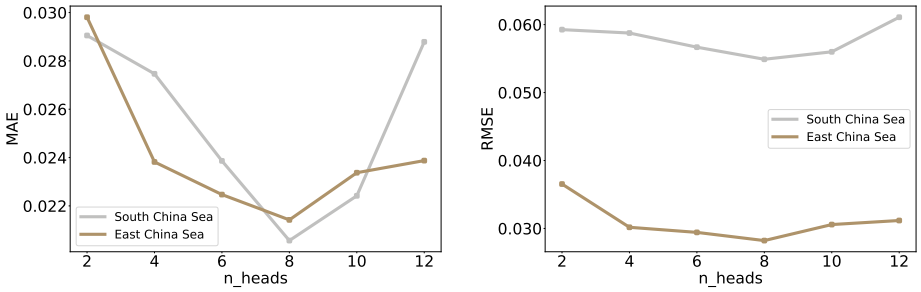

((a)) MAE ((b)) RMSE

Figure 1: The results of SMO-STANet while varying the hyper-parameter *n_heads*.

A.2 The impacts of parameter decay_factor η on the performance of SMO-STANet

we have conducted experiments to evaluate the impacts of parameter decay_factor η on the performance of SMO-STANet to determine their optimal values. According to the Figure 2, we set η to 1.5 and 1.0 for East China Sea dataset and South China Sea dataset, respectively, to achieve the optimal performance.

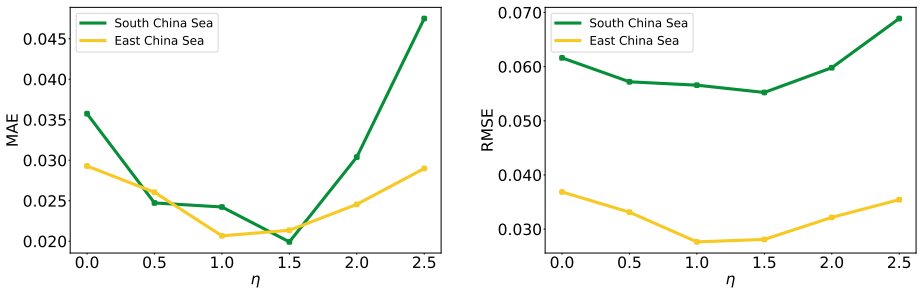

((a)) MAE ((b)) RMSE

Figure 2: The results of SMO-STANet while varying the hyper-parameter η in the scaled loss function.

A.3 The impacts of parameter seq_len on the performance of SMO-STANet

we have conducted experiments to evaluate the impacts of parameter seq_len on the performance of SMO-STANet to determine their optimal values. According to the Figure 3, we set seq_len to 32 to achieve the optimal performance.

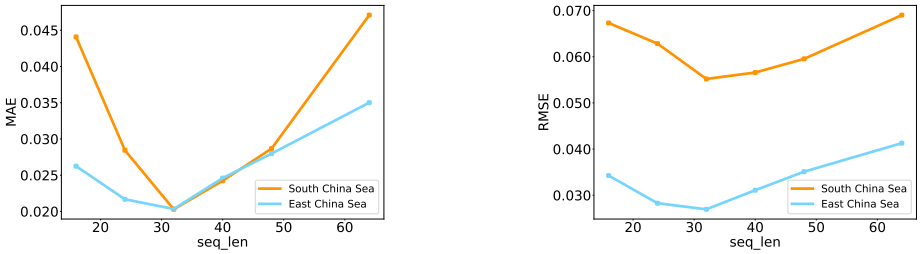

((a)) MAE ((b)) RMSE

Figure 3: The results of SMO-STANet while varying the sequence length *seq_len*.

A.4 The impacts of parameter pred_len on the performance of SMO-STANet

As illustrated in Figure 4, we have analyzed how the variations in pred_len influence the predictive performance of SMO-STANet. Based on the results, we can see that when seq_len is constant, the prediction performance becomes worse as pred_len becomes longer.

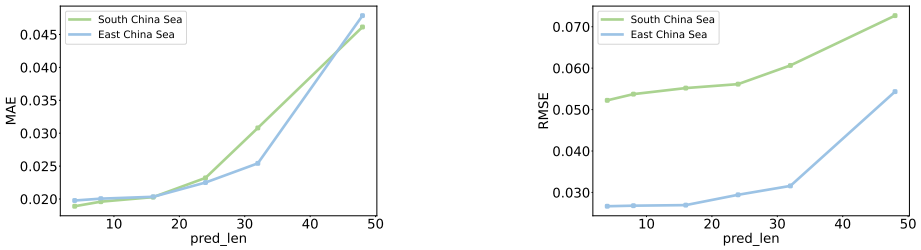

((a)) MAE ((b)) RMSE

Figure 4: The results of SMO-STANet while varying the prediction length *pred_len*.

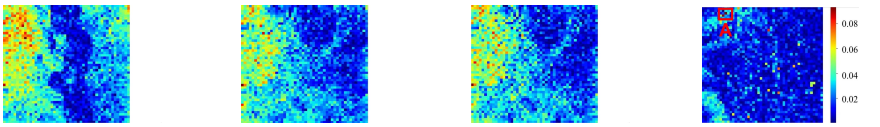

(a) LSTM (b) Transformer (c) Informer (d) SMO-STANet

Figure 5: The MAE visualization of Chl-a prediction in the East China Sea on June 6, 2022.

B Visualization of the performance of SMO-STANet

Figures 5 and 6 visualize the MAE distributions of different Chl-a prediction methods in the two study areas.

The visualization reveals that MAE of SMO-STANet is obviously smaller than the other three baseline methods, which indicates the superiority of SMO-STANet. Notably, SMO-STANet does not perform well in some small areas include the highlighted region A in the East China Sea, and highlighted regions B in the South China Sea. Our findings indicate that these regions are influenced by the Kuroshio warm current, resulting in large fluctuations in Chl-a, ultimately degrading prediction performance.

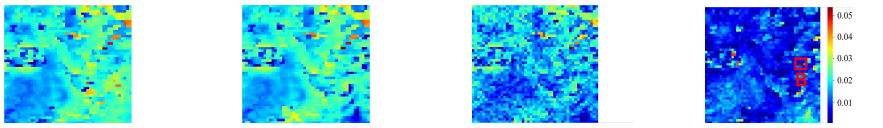

(a) LSTM (b) Transformer (c) Informer (d) SMO-STANet

Figure 6: The MAE visualization of Chl-a prediction in the South China Sea on June 18, 2022.